Environmental Science and Pollution Research (2019) 26:15229–15247
https://doi.org/10.1007/s11356-019-04875-y

RESEARCH ARTICLE

Numerical model of aerobic bioreactor landfill considering aerobic-anaerobic condition and bio-stable zone development

Shi-Jin Feng[1] · An-Zheng Li[1] · Qi-Teng Zheng[1] · Ben-Yi Cao[2] · Hong-Xin Chen[1]

Received: 10 January 2019 / Accepted: 13 March 2019 / Published online: 30 March 2019

Abstract

Aeration by airflow technology is a reliable method to accelerate waste biodegradation and stabilization and hence shorten the aftercare period of a landfill. To simulate hydro-biochemical behaviors in this type of landfills, this study develops a model coupling multi-phase flow, multi-component transport and aerobic-anaerobic biodegradation using a computational fluid dynamics (CFD) method. The uniqueness of the model is that it can well describe the evolution of aerobic zone, anaerobic zone, and temperature during aeration and evaluate aeration efficiency considering aerobic and anaerobic biodegradation processes. After being verified using existing in situ and laboratory test results, the model is then employed to reveal the bio-stable zone development, aerobic biochemical reactions around vertical well (VW), and anaerobic reactions away from VW. With an increase in the initial organic matter content (0.1 to 0.4), the bio-stable zone expands at a decreasing speed but with all the horizontal ranges larger than 17 m after an intermittent aeration for 1000 days. When waste intrinsic permeability is equal or greater than 10^{-11} m^2, aeration using a low pressure between 4 and 8 kPa is appropriate. The aeration efficiency would be underestimated if anaerobic biodegradation is neglected because products of anaerobic biodegradation would be oxidized more easily. A horizontal spacing of 17 m is suggested for aeration VWs with a vertical spacing of 10 m for screens. Since a lower aeration frequency can give greater aeration efficiency, a 20-day aeration/20-day leachate recirculation scenario is recommended considering the maximum temperature over a reasonable range. For wet landfills with low temperature, the proportion of aeration can be increased to 0.67 (20-day aeration/10-day leachate recirculation) or an even higher value.

Keywords Bioreactor landfill · Aeration · Leachate recirculation · CFD · Stabilization

Responsible editor: Marcus Schulz

✉ Hong-Xin Chen
chenhongxin@tongji.edu.cn

Shi-Jin Feng
fsjgly@tongji.edu.cn

An-Zheng Li
1710696@tongji.edu.cn

Qi-Teng Zheng
08qitengzheng@tongji.edu.cn

Ben-Yi Cao
bc457@cam.ac.uk

[1] Key Laboratory of Geotechnical and Underground Engineering of the Ministry of Education, Department of Geotechnical Engineering, Tongji University, Shanghai 200092, China

[2] Department of Engineering, University of Cambridge, Trumpington Street, Cambridge CB2 1PZ, UK

Introduction

Landfills are the most widely used facility for disposing municipal solid waste (MSW) all around the world. It generally takes a long period of time and a high cost of post-closure aftercare for these landfills to reach biological stabilization state. To promote waste stabilization, one of the common technologies is to introduce additional air (or moisture) into landfills, which are called aerobic (or anaerobic) bioreactor landfills. Compared with anaerobic reaction, organic matters in aerobic condition can be degraded more completely at a much higher reaction rate, giving a better leachate quality as well (Grisey and Aleya 2016; Liu et al. 2018a). Therefore, this technique attracts increasing attention in recent years and has been successfully applied to several landfills in Europe (Raga et al. 2015; Ritzkowski et al. 2016), North America (Ko et al. 2013), Austria (Hrad and Huber-Humer 2017), and Asia (Liu et al. 2018b).

MSW is composed of leachate, gas, and solid skeleton. Leachate-gas flow in landfill is essentially a process of coupled multi-phase fluid flow in porous media and has been simulated using various tools (e.g., Reddy et al. 2012; Ng et al. 2015; Feng et al. 2017a). Since anaerobic landfills are more common, great efforts have been made to simulate the hydro-biochemical processes in this type of landfill (McDougall 2007; White 2008; Hubert et al. 2016; Feng et al. 2018; Park et al. 2018). Overall, researches of anaerobic landfills are relatively advanced in the past decade.

On the other hand, some efforts have also been made to simulate the hydro-biochemical behaviors of MSW under aerobic condition. Haarstrick et al. (2004) proposed a biochemical model for waste biodegradation which can simulate the fate of carbon compounds in aerobic or anaerobic condition. Kim et al. (2007) created a more realistic compartment model for waste biodegradation considering heat generation and the fate of nitrogen and carbon compounds in aerobic or anaerobic condition. However, the above two models cannot consider the spatial hydro-biochemical behavior in a large zone. To explore the spatial hydro-biochemical behavior, Fytanidis and Voudrias (2014) developed a numerical model for landfill aeration by vertical wells (VWs) considering multi-phase flow and multi-component transport, but a one-stage aerobic biodegradation model was adopted which would underestimate the aeration efficiency. Omar and Rohani (2017) simulated the conversion of a landfill which was operated from anaerobic condition to aerobic condition, but the model is one-dimensional (1D) with a constant organic content. Cao et al. (2018) adopted a two-stage aerobic and anaerobic biodegradation model to study the hydro-biochemical processes in a 3D aerobic-anaerobic hybrid bioreactor landfill. However, they artificially stopped the anaerobic degradation during aeration and neglected heat production and transfer, which gives rise to a grave concern of high temperature and explosion risk in an aerobic landfill. Until now, no numerical model can address all the abovementioned shortcomings, and hence, the development of aerobic zone in anaerobic environment is still unclear as well as temperature distribution and aeration efficiency.

The first objective of this paper is to develop a numerical model which couples aerobic-anaerobic biodegradation, multi-phase flow, multi-component transport, and heat transfer. The second objective is to give insight into the development of aerobic zone in anaerobic environment. The final objective is to investigate the effects of waste properties (initial content of organic matters and intrinsic permeability) and aeration design parameters (pressure, well depth, and frequency) on hydro-biochemical behaviors during aeration in terms of aeration efficiency and influence zone.

Model development

VW is one of the most widely used methods of low pressure aeration (normally 2 kPa to 8 kPa), especially for old landfills to accelerate the landfill stabilization (Ritzkowski and Stegmann 2012). As shown in Fig. 1a, a low-permeability cover system is used to isolate the flow to the atmosphere; thus, the top surface of the landfill is simplified as a zero flux boundary. Given the periodically spaced VWs, the lateral boundary is assumed as impermeable for leachate and gas. The bottom is set as a free drainage boundary to enable the leachate collection by the leachate collection and removal system (LCRS) with 3% slope. The landfill height and VW depth are H_0 and H_w, respectively. There is an uprated machine at the landfill surface which can provide the motive force for air compression and injection, and the air is injected into the landfill through a H_s long screen at the bottom of VW.

Under normal waste disposal condition, an anaerobic environment is dominant in landfill. With the air addition, the anaerobic zone around air injection wells is switched to an aerobic environment first because of the expansion of oxygen. The organic matters in waste and products of anaerobic biodegradation can both react with oxygen. Thus, both aerobic and anaerobic reactions exist in an aerobic bioreactor landfill, and which one happens in a specific area depends on the oxygen pressure (Kim et al. 2007). In the rest part of this section, the governing equations for multi-phase flow, multi-component transport, and aerobic-anaerobic biodegradation will be introduced, followed by the solution procedures.

Multi-phase flow equations

The governing equations of multi-phase flow are formulated by introducing the concept of phasic volume fraction (α_q), which represents the ratio of the volume occupied by phase q (V_q) to the total void volume. V_q can be described as follows:

$$V_q = \int_V \alpha_q dV \tag{1}$$

where

$$\sum_{q=\text{leachate,gas}} \alpha_q = 1 \tag{2}$$

For phase q, the mass continuity equation is expressed as

$$\frac{\partial}{\partial t}\left(n\alpha_q\rho_q\right) + \nabla\cdot\left(n\alpha_q\rho_q\overrightarrow{v_q}\right) = nS_q \tag{3}$$

where n is the total porosity of MSW (dimensionless), ρ_q is the density of phase q (kg m^{-3}), t is the time (s), $\overrightarrow{v_q}$ is the velocity of phase q (m s^{-1}), and S_q is the source/sink term of phase q (kg m^{-3} s^{-1}).

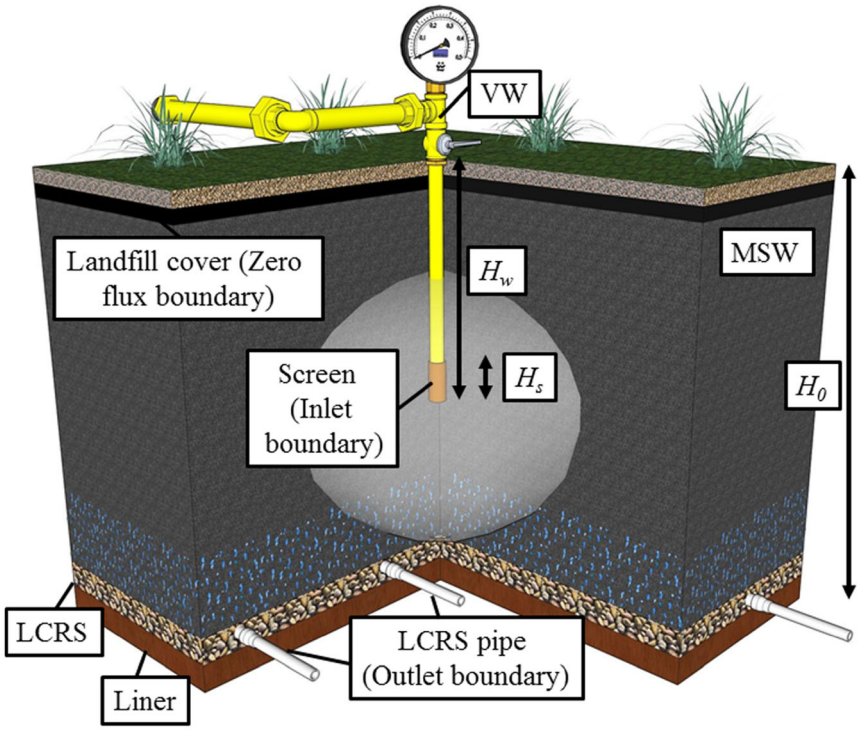

(a)

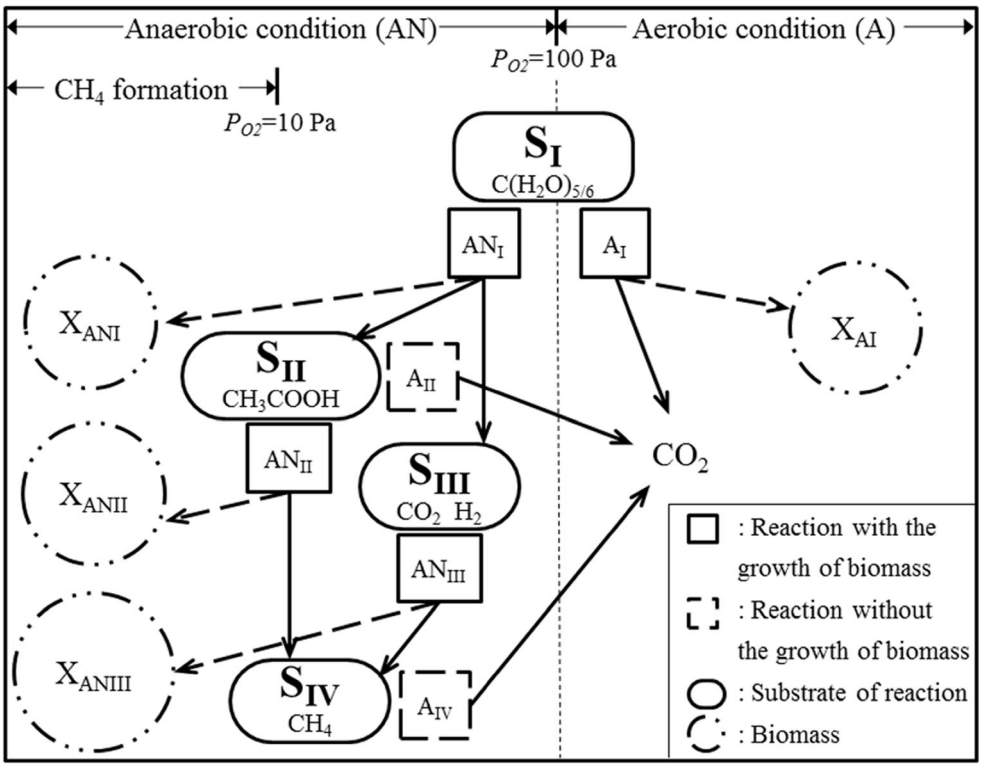

I ~ IV: reaction processes

S_I ~ S_{IV}: Substrate X: Biomass A: Aerobic reactions AN: Anaerobic reactions

(b)

Fig. 1 **a** Schematic diagram of aerobic bioreactor landfill with aeration well. **b** Biodegradation processes in the landfill

The momentum conservation for phase q is described as

$$\frac{\partial}{\partial t}\left(n\alpha_q\rho_q\overrightarrow{v_q}\right)+\nabla\cdot\left(n\alpha_q\rho_q\overrightarrow{v_q}\overrightarrow{v_q}\right)$$
$$=-n\alpha_q\nabla p_q+\nabla n\overline{\overline{\tau}}+n\alpha_q\rho_q\overrightarrow{g}-\alpha_q^2\frac{\mu_q}{k_{\mathrm{i}}k_{\mathrm{r}}}\overrightarrow{v_q}-n\alpha_q\nabla p_c \quad (4)$$

where p_q is the pressure for phase q (Pa; l for leachate and g for gas), p_c is the capillary pressure (Pa), $\overline{\overline{\tau}}$ is the shear stress tensor (Pa), g is the acceleration of gravity (m s^{-2}), μ_q is the dynamic viscosity of phase q (kg m^{-1} s^{-1}), k_{i} is the intrinsic permeability (m^2), and k_{r} is the relative permeability (dimensionless).

The capillary pressure term $n\alpha_q\nabla p_c$ only exists in the equation of leachate phase, and p_c can be described by the van Genuchten-Mualem (VGM) model (Reichenberger et al. 2006):

$$p_c=-\frac{\rho_l g}{\alpha_{vg}}\left(S_e^{-\frac{1}{m_{\mathrm{vg}}}}-1\right)^{\frac{1}{n_{\mathrm{vg}}}} \quad (5)$$

where ρ_{l} is the density of leachate phase (kg m^{-3}), α_{vg} is the VGM parameter related to the air entry pressure (Pa^{-1}), m_{vg} and n_{vg} are the van Genuchten constants, and S_{e} is the effective degree of saturation which can be expressed as

$$S_e=\frac{\alpha_l-\alpha_{lr}}{\alpha_{ls}-\alpha_{lr}} \quad (6)$$

where α_{l}, α_{lr}, and α_{ls} are the volume fraction, residual volume fraction, and maximum volume fraction of leachate phase, respectively.

To describe the conservation of energy in Eulerian multiphase applications, this study adopts a separate enthalpy equation for each phase

$$\frac{\partial}{\partial t}\left(\alpha_q\rho_q h_q\right)+\nabla\cdot\left(n\alpha_q\rho_q h_q\overrightarrow{v_q}\right)=\alpha_q\frac{\partial\rho_q}{\partial t}+\overline{\overline{\tau}}$$
$$:\nabla\overrightarrow{v_q}-\nabla\overrightarrow{q_q}+\sum R_{\bullet}^{i}(-\Delta H_b)_{\bullet}^{i}+Q_{pq} \quad (7)$$

where h_q is the specific enthalpy of phase q, $\overrightarrow{q_q}$ is the heat flux, $R_{\bullet}^{i}$ is the reaction rate (kmol day^{-1} m^{-3}), ΔH_{b} is the reaction heat (MJ kmol^{-1}) (Table 1), and Q_{pq} is the intensity of heat exchange between phases.

Multi-component transport equations

In this study, leachate phase contains five components: volatile fatty acid (CH_3COOH) abbreviated as VFA and four kinds of biomass ($CH_{1.5}O_{0.3}N_{0.24}$), and gas phase contains four components: O_2, CO_2, CH_4, and N_2. A convection-diffusion equation is adopted herein to describe the transport of these components

$$\frac{\partial}{\partial t}\left(\rho_q Y_i\right)+\nabla\cdot\left(\rho_q\overrightarrow{v_q}Y_i\right)=-\nabla\cdot\overrightarrow{J_i}+R_i \quad (8)$$

where Y_i represents the mass fraction of component i in phase q, R_i is the source/sink term of component i in biochemical reactions (kg m^{-3} s^{-1}), and $\overrightarrow{J_i}$ is the diffusion flux of component i due to the concentration gradient, and the mass diffusion is modeled using Fick's law:

$$\overrightarrow{J_i}=-\rho_q D_i\nabla Y_i-D_{T,i}\frac{\nabla T}{T} \quad (9)$$

where D_i is the mass diffusion coefficient for component i in the mixture, $D_{T,i}$ is the thermal diffusion coefficient, and T is the temperature.

Aerobic-anaerobic biodegradation

As mentioned earlier, Kim et al. (2007) proposed a comprehensive compartment model of the biodegradation of organic matters in aerobic, anaerobic, or semi-aerobic landfills, which switches between anaerobic and aerobic conditions depending on the local oxygen pressure. This model has proved to be able to well describe the hydro-biochemical behaviors of MSW. This study combines it with a computational fluid dynamics (CFD) technique to model the spatial hydro-biochemical behaviors during aeration. Anaerobic reactions and aerobic reactions in Fig. 1b are termed as "AN" and "A", respectively. These reactions can be classified into three categories: hydrolysis (termed as AN_I), methanation from VFA (termed as AN_{II}) and from CO_2 and H_2 (termed as AN_{III}), and oxidation from organic matter (termed as A_I), from VFA (termed as A_{II}), and from CH_4 (termed as A_{IV}). The subscripts represent substrates of each reaction, namely "I" for organic matter, "II" for VFA, "III" for CO_2 and H_2, and "IV" for CH_4. In Table 1, negative and positive stoichiometric coefficients indicate reactants and products. Waste is viewed as an assembly of solid, liquid, and gas phases. The solid phase is divided into degradable organic matter and undegradable part, and the degradable organic matter is simplified as $C(H_2O)_{5/6}$ from a perspective of cellulose. In leachate phase, the growth of biomass depends on substrates of reactions (A_I, AN_I, AN_{II}, and AN_{III}) and partial pressure of O_2, and some reactions (A_{II} and A_{IV}) occur independent of biomass.

Reactions with biomass growth

For concentrations of substrates $C(H_2O)_{5/6}$ (termed as S_I) (kmol m^{-3} cell), CH_3COOH (termed as S_{II}) (kmol m^{-3} liquid),

Table 1 Stoichiometric coefficients of biochemical reactions from Kim et al. (2007)

Reaction	A_I	AN_I	A_{II}	AN_{II}	AN_{III}	A_{IV}	A-biomass decay	AN-biomass decay	Methanogenic biomass decay
$C(H_2O)_{5/6}$	− 1	− 1							
$CH_{1.5}O_{0.3}N_{0.24}$	$+Y_{AI}$	$+Y_{ANI}$		$+Y_{ANII}$	$+Y_{ANIII}$		− 1	− 1	− 1
O_2	− 0.687		− 1			− 2	− 1.045		
H_2O	+ 0.716	− 0.493	+ 2	+ 0.033	+ 1.985	+ 1	+ 0.390	− 1.700	− 0.655
CH_3COOH		+ 0.167	− 1	− 0.5				+ 0.500	
CO_2	+ 0.700	+ 0.467	+ 2	+ 0.476	− 1	+ 1	+ 1	+ 0.5	+ 0.478
H_2		+ 1.203			− 3.905			+ 1.090	
CH_4				+ 0.474	+ 0.950	− 1			+ 0.673
NH_3	− 0.072	− 0.240		− 0.012	− 0.012		+ 0.24	+ 0.24	+ 0.24
$-\Delta H_b$ (MJ kmol^{-1})	+ 460	+ 110	+ 460	− 16	+ 250		+ 460	+ 36	+ 46.3

and CO_2 and H_2 (termed as S_{III}) (kmol m^{-3} gas), their temporal changes can be formulated as

$$\frac{dS_I}{dt} = -\frac{R^G_{AI}}{Y_{AI}} \tag{10}$$

$$\frac{dS_I}{dt} = -\frac{R^G_{ANI}}{Y_{ANI}} \tag{11}$$

$$\alpha_l \frac{dS_j}{dt} = -\frac{R^G_{ANj}}{Y_{ANj}} \quad (j = II, III) \tag{12}$$

where R^G_{AI} and R^G_{ANI} are the growth rates of biomass for the reactions "A_I" and "AN_I" (kmol day^{-1} m^{-3} cell), R^G_{ANj} is the growth rate of biomass for S_j under an anaerobic (subscript "ANj") environment (kmol day^{-1} m^{-3} cell), and $Y_{\cdot}$ represents the yield coefficient with subscripts of AI, ANI, and ANj for different scenarios (dimensionless) (Kim et al. 2007) (Table 2).

The growth rates of biomass are expressed as

$$R^G_{AI} = \eta_{AI}\mu_{AI}X_{AI} \tag{13}$$

$$R^G_{ANj} = \eta_{ANj}\mu_{ANj}X_{ANj} \quad (j = I, II, III) \tag{14}$$

where $\mu_{\cdot}$, $X_{\cdot}$, and $\eta_{\cdot}$ are the specific growth rate of biomass (day^{-1}), the concentration of biomass (kmol m^{-3} cell), and the environmental inhibition factor with different subscripts representing different scenarios. For example, μ_{ANj} is the specific growth rate of biomass for S_j under an anaerobic environment (day^{-1}). The environmental inhibition factor $\eta_{\cdot}$ is estimated by multiplying the temperature factor (f_T) and moisture content factor (f_θ) (Kim et al. 2007)

$$f_T = \begin{cases} 0 & (T < 293.15\,\mathrm{K}) \\ e^{-6150/T}/e^{-6150/303} & (293.15\,\mathrm{K} \le T < 313.15\,\mathrm{K}) \\ 1.9 & (313.15\,\mathrm{K} \le T < 323.15\,\mathrm{K}) \\ 1.9 \times e^{-7460/T}/e^{-7460/323} & (323.15\,\mathrm{K} \le T < 333.15\,\mathrm{K}) \\ 3.8 & (333.15\,\mathrm{K} \le T < 343.15\,\mathrm{K}) \\ 3.8 \times e^{110{,}000/T}/e^{110{,}000/343} & (343.15\,\mathrm{K} \le T < 348.15\,\mathrm{K}) \\ 0 & (348.15\,\mathrm{K} \le T) \end{cases} \tag{15}$$

$$f_\theta = \begin{cases} 0 & (\alpha_l < 0.1) \\ (\alpha_l - 0.1) \times 10 & (0.1 \le \alpha_l < 0.2) \\ 1.0 & (0.2 \le \alpha_l) \text{ for reaction } AN_j \\ 1.0 & (0.2 \le \alpha_l < 0.35) \text{ for reaction } A_I \\ 3.33 - \alpha_l \times 6.67 & (0.35 \le \alpha_l < 0.5) \text{ for reaction } A_I \\ 0 & (0.5 \le \alpha_l) \text{ for reaction } A_I \end{cases} \tag{16}$$

Table 2 Parameters for biochemical reactions from Kim et al. (2007)

Reaction process	μ_{max} (day^{-1})	Y	K	k_{O_2} (MPa)	k
A_I	1.0	0.3		0.02 × 0.1013	6.7 (kmol m^{-3} cell)
AN_I	0.02	0.2			1.7 (kmol m^{-3} cell)
A_{II}			0.005 (kmol day^{-1} m^{-3} liquid)	0.02 × 0.1013	0.02 (kmol m^{-3} liquid)
AN_{II}	0.2	0.05			0.05 (kmol m^{-3} liquid)
AN_{III}	0.2	0.05			0.3 × 0.1013 (Pa)
A_{IV}			6.48 × 10^{-5} (kmol day^{-1} kg^{-1})	0.012 × 0.1013	

Based on the Monod model, the specific growth rates (μ_{AI} and μ_{ANj}) can be expressed as

$$\mu_{AI} = \mu_{AI}^{max}\frac{S_I}{k_{AI}+S_I}+\frac{P_{O_2}}{k_{O_2,I}+P_{O_2}} \quad (17)$$

$$\mu_{AN_j} = \mu_{AN_j}^{max}\frac{S_j}{k_{AN_j}+S_j} \quad (j=I,II) \quad (18)$$

$$\mu_{ANIII} = \mu_{ANIII}^{max}\frac{P_{H_2}}{k_{ANIII}+P_{H_2}} \quad (19)$$

where $\mu_{\bullet}^{max}$ is the maximum specific growth rate (day^{-1}); k_{AI}, k_{AN_j}, and k_{ANIII} are the Monod saturation constants under aerobic condition (subscript AI) and anaerobic condition (subscripts AN*j* and ANIII); $k_{O_2,I}$ is the O_2 saturation constant for $C(H_2O)_{5/6}$ (termed as S_I) (Table 2); and P_{O_2} and P_{H_2} are the partial pressures of O_2 and H_2 (Pa) (Kim et al. 2007).

Growth and decay of biomass

The change rate of biomass in each reaction is

$$\frac{dX_\bullet}{dt} = R_\bullet^G - R_\bullet^D \quad (\bullet = A_I, AN_I, AN_{II}, AN_{III}) \quad (20)$$

where $R_\bullet^D$ is the decay rate of biomass (kmol day^{-1} m^{-3} cell) (Kim et al. 2007)

$$R_\bullet^D = 0.05\bullet\mu_\bullet^{max}\left(X_\bullet - X_\bullet^{ini}\right) \quad (\bullet = A_I, AN_I, AN_{II}, AN_{III}) \quad (21)$$

where $X_\bullet^{ini}$ represents the initial concentration of biomass (kmol m^{-3} cell).

Reactions without biomass growth

Reactions A_{II} and A_{IV} are described by the Michaelis-Menten kinetics as

$$\frac{dS_{II}}{dt} = \frac{K_{AII}S_{II}}{k_{AII}+S_{II}}\frac{P_{O_2}}{k_{O_2,II}+P_{O_2}} \quad (22)$$

$$\frac{dS_{IV}}{dt} = -\eta_{AIII}\frac{K_{AIII}P_{CH4}}{k_{P_{CH4}}+P_{CH4}}\frac{P_{O_2}}{k_{O_2,IV}+P_{O_2}} \quad (23)$$

where $K_\bullet$ is the reaction rate constant for VFA oxidation (subscript AII) (kmol day^{-1} m^{-3} liquid) or methane oxidation (subscript AIV) (kmol day^{-1} kg^{-1}) (Table 2); k_{AII} is the Monod saturation constant of oxidation reaction of VFA; P_{CH_4} and k_{CH_4} are the partial pressure of CH_4 (Pa) and the saturation constant for CH_4, respectively; and $k_{O_2,II}$ and $k_{O_2,IV}$ are the O_2 saturation constants for CH_3COOH (termed as S_{II}) and CH_4 (termed as S_{IV}), respectively. η_{AIII} is the environmental inhibition factor considering f_T and f_θ (Ng et al. 2015) as follows:

$$f_T = \begin{cases} 0.0142T & (T < 288.15\ K) \\ 0.112T-1.47 & (288.15\ K \le T < 306.15\ K) \\ 2.235-0.18(T-33) & (306.15\ K \le T) \end{cases} \quad (24)$$

$$f_\theta = \begin{cases} 0 & (\alpha_l < 0.25) \\ \frac{n\alpha_l-0.15}{0.2-0.15} & (0.25 \le \alpha_l < 0.33) \\ 1 & (0.33 \le \alpha_l) \end{cases} \quad (25)$$

Solution procedures

This model is solved by utilizing the CFD technique based on the ANSYS Fluent platform (ANSYS 2009). User-defined functions (UDFs) are embedded into the platform to define the aerobic/anaerobic biodegradation processes. A segregated solver and a pressure-velocity coupling method are adopted. First, based on the initial pressure, the momentum conservation equation (Eq. 4) is solved to update velocity. Then, the continuity equation (Eq. 3) is solved to correct pressure. Finally, the energy conservation equation (Eq. 7), multicomponent transport equations (Eqs. 8 and 9), and aerobic-anaerobic biodegradation equations (Eqs. 10–25) are solved. The detailed solving procedures are shown in Fig. 2. In this model, if the scaled residuals of variables in all the governing equations decrease to 10^{-3}, the convergence criteria are satisfied. The expression and monitoring method of scaled residual are concretely introduced in ANSYS (2009).

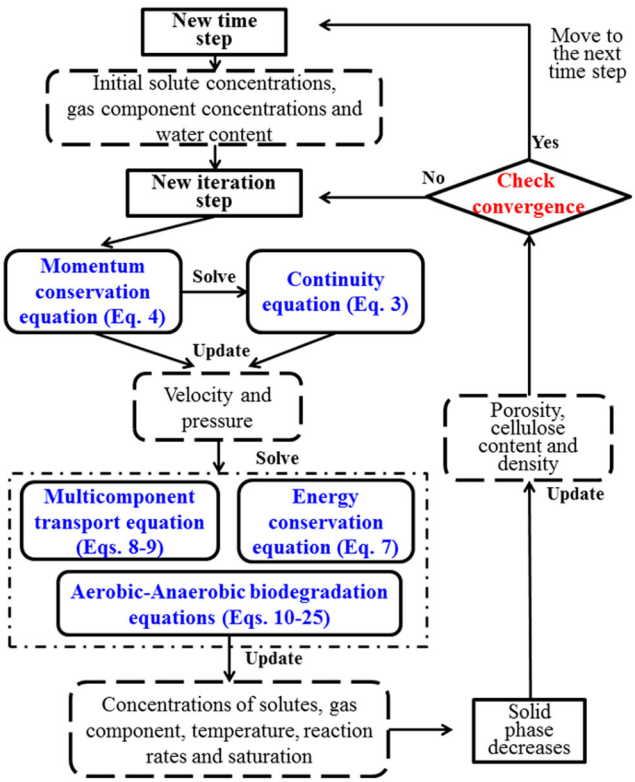

Fig. 2 Solution procedures of the model

Model verification

Liu et al. (2018b) monitored the partial pressures of O_2 and CH_4 and temperature in the first aerobic landfill in China. The reported in situ data is adopted to test the performance of the present model. The MSW was 14 m thick and covered by a 3-m-thick clay layer as the final cover, and the air injection rate was 93 $m^3\ h^{-1}$ for single well. Herein, the aeration system is simplified as an axisymmetric model with air injection well. The well has a depth of 14 m from the final cover surface, a diameter of 5 cm, and a screen length of 1 m. The initial concentrations of biomass and VFA, which were not provided by Liu et al. (2018b), are adopted from Table 3. The other needed parameters are enclosed in Table 4 and Fig. 3. The lateral boundary is fixed at the atmospheric pressure to simulate the gas collection system. As shown in Fig. 3, the partial pressures of O_2 and CH_4 and temperature calculated by the proposed model agree with the reported data reasonably well.

Since the detailed biodegradation information was not reported by Liu et al. (2018b), the laboratory experimental data reported by Lavagnolo et al. (2018) is adopted to verify the performance of the present model in describing aerobic-anaerobic biodegradation processes. They filled waste in two lysimeters (height of 1 m, inner diameter of 24 cm) and monitored the partial gas pressures under anaerobic and aerobic conditions for about 90 days, respectively. The lysimeters were irrigated with a rate of 0.9 L day^{-1}. Similarly, the initial concentrations of biomass and VFA are adopted from Table 3, and the other needed parameters are enclosed in Table 4 and Fig. 4. The partial pressures of CH_4, CO_2, and O_2 calculated by this model closely match the data of Lavagnolo et al. (2018) (Fig. 4). There is a difference in the partial pressure of CO_2 under an anaerobic condition during the first 30 days (Fig. 4a) because the waste used for the laboratory test came from an aerobic environment, giving a short-term aerobic biodegradation process in the first 30 days. Thus, the proposed model can reasonably simulate complicated hydro-biochemical processes in an aerobic bioreactor landfill and is now used to investigate the influences of some important factors in the following part.

Results and discussion

Input information

The computational domain is axisymmetric with a height (H_0) of 30 m and a radius of 40 m (Fig. 5a). A VW is placed at the center of the computational domain for aeration and its depth (H_w = 0.4 and H_0 = 12 m) unless focusing on the influence of VW depth. The screen length of VW (H_s) is equal to 1.2 m, and the well diameter (d) is equal to 0.15 m (Ko et al. 2013; Liu et al. 2018b). In this study, intermittent aeration of 10-day aeration/10-day leachate recirculation is used with the aeration duration equal to half of the total period unless when exploring the impact of operation manner. The computational domain is discretized into grid with a cell size ranging from 0.01 to 2.11 m^2. The initial mass fraction of cellulose before aeration (C_0) is assumed as 0.3 to represent an old landfill reaching the final stage of anaerobic biodegradation. An anisotropy coefficient (A) of 10 is adopted here, defining the ratio of horizontal intrinsic permeability (k_h) to vertical intrinsic permeability (k_v) (Stoltz et al. 2010). The other needed input parameters are summarized in Tables 2, 3, and 4.

Influence of aerobic biodegradation

This model adopts an aerobic-anaerobic biodegradation module to investigate the evolution of anaerobic zone (P_{O_2} is lower than 100 Pa) and aerobic zone (P_{O_2} is greater than 100 Pa) during aeration, which has not been studied in previous studies. As shown in Fig. 5a, the aerobic zone consists of two

Table 3 Biochemical parameters for landfill

Parameter	Value	Reference
Initial concentration of VFA (kg m^{-3} liquid)	1.00	McDougall (2007)
Initial partial pressure of CO_2 in gas phase (%)	50.0	Hrad and Huber-Humer (2017)
Initial partial pressure of CH_4 in gas phase (%)	50.0	
Initial partial pressure of O_2 in gas phase (%)	0	
Initial partial pressure of N_2 in gas phase (%)	0	
Initial mass fraction of $C(H_2O)_{5/6}$	0.3	Kim et al. (2007)
Initial concentration of $CH_{1.5}O_{0.3}N_{0.24}$	$X_{AI} = 0.1Y_{AI}S_I$ $X_{ANI} = 0.01Y_{ANI}S_I$ $X_{ANi} = 0.0095Y_{ANi}S_i$ (i = II, III)	
Initial temperature of landfill (K)	308.15	Liu et al. (2018b)

Table 4 Hydraulic parameters adopted in this study

Parameter	Value	Reference
Density of MSW (kg m^{-3})	600	Powrie and Beaven (1999); Stoltz et al. (2010)
k_v (m^2)	1.0×10^{-10}~1.0×10^{-13}	
A	10	
n	0.6	White et al. (2015)
n_{vg}	2.4	
m_{vg}	0.58	
α_{vg} (kPa^{-1})	1.5	
α_l	0.2	
α_{lr}	0.15	

parts: one is the bio-stable zone, where the cellulose has been largely degraded, and the other is the S_I oxidation zone, where the A_I reaction is quite active. The bio-stable zone can be explained by a much faster rate (almost five times) of aerobic degradation (a maximum rate of about 1.3×10^{-5} kg m^{-3} s^{-1}) than that of anaerobic degradation (a maximum rate of about 2.8×10^{-6} kg m^{-3} s^{-1}). As air injection continues, the increase in oxygen concentration expands the aerobic zone into the anaerobic zone (Fig. 5a, b). Figure 5c gives the migration of the recirculated leachate which flows downwards under gravity with time. At around $t = 600$ days, the recirculated leachate reaches the bottom and moves along the bottom slope before being collected by the LCRS (marked by "Outlet").

Figure 6 also gives the distribution of partial pressure of each component (O_2, CO_2, and CH_4), which can reflect the distribution of each reaction rate. After aeration for 200 days, partial pressure of O_2 reaches 0.21 in the bio-stable zone (red zones in Fig. 6a) as the cellulose in this area has been largely oxidized and the consumption of O_2 is rather weak. At the edge of aerobic zone, oxygen concentration declines gradually. The reason is that with the expansion of aerobic zone, the cellulose, VFA, and methane in the anaerobic zone are exposed to oxygen, inducing oxidation reactions (A_I, A_{II}, and A_{IV}). The partial pressures of CH_4 and CO_2 in most part of anaerobic zone (red zone in Fig. 6c) are both about 50% which agree well with in situ results (Hrad and Huber-Humer 2017), except for a higher partial pressure of CO_2 at the edge of the zone (e.g., red zone in Fig. 6b). It increases because the CH_4 produced by methanation (AN_{II} and AN_{III}) is oxidized (A_{IV}) at the edge of anaerobic zone but the amount of CO_2 remains unchanged.

Influence of initial organic matter content

Aeration is mostly applied to old landfills where the anaerobic process of waste comes to the end and the remaining amount of degradable organic matters would directly affect the required duration of aeration. Kitchen waste plays an essential role in the waste compositions in China, but paper, wood, and fiber dominate in most developed countries (Townsend et al. 2015; Feng et al. 2017b). Therefore, to consider the difference of waste composition in different countries, four values of initial mass fraction of cellulose for aeration C_0 (0.1, 0.2, 0.3, and 0.4) are adopted for studying its influence on the horizontal range of bio-stable zone (D_{hs}). The bio-stable zone expands over time, and the expansion speed increases with decreasing C_0 given the same elapsed time (Fig. 7). For example, a C_0 of 0.1 needs much less time for D_{hs} reaching 15 m (400 days) than a C_0 of 0.4 (800 days). Besides, the bio-stable zone expands slowly after aeration for about 400 days. For example, when C_0 is equal to 0.1, the D_{hs} reaches 15 m for the first 400 days and increases by 5 m for 600 more days. Therefore, C_0 is important for operators to properly design aeration time and horizontal spacing of aeration wells. If C_0 is equal to 0.3, the cellulose content at 1 m horizontally away from the well screen rapidly decreases to zero within 30 days because the area near the aeration inlet is in an optimal aerobic environment. However, for the area located at 10 m horizontally away, its cellulose content slowly decreases following anaerobic reactions in the first 200 days and, after that, it is completely oxidized within 80 days due to the arrival of the injected oxygen. The gradients of the curve before and after 200 days represent the anaerobic and aerobic degradation rates which prove a much higher consumption rate of cellulose in the aerobic environment.

Figure 8 depicts the temporal changes in the mass fraction of cellulose, concentrations of VFA and biomass for hydrolysis from cellulose (X_{ANI}), and methanation from VFA (X_{ANII}) in the area which is located at 40 m horizontally away from the well screen, giving a completely anaerobic environment. For $C_0 = 0.4$, the mass fraction of cellulose decreases by 0.4 to 0.3 for 336 days of anaerobic reactions, to 0.2 for 224 more days, and finally, to 0.1 for 382 more days, which give an average value of 314 days for a decrease of 0.1 in the mass fraction of cellulose in an anaerobic environment (Fig. 8a). A value of 224 days implies faster anaerobic degradation of cellulose from a mass fraction of 0.3 to 0.2 than that from 0.4 to 0.3 and from 0.2 to 0.1. The reason is that the hydrolysis biomass (X_{ANI}) increases over time to a peak value of 0.42 mol L^{-1} in the first 350 days and, after that, it decreases due to a decrease in cellulose content. The concentration of VFA increases

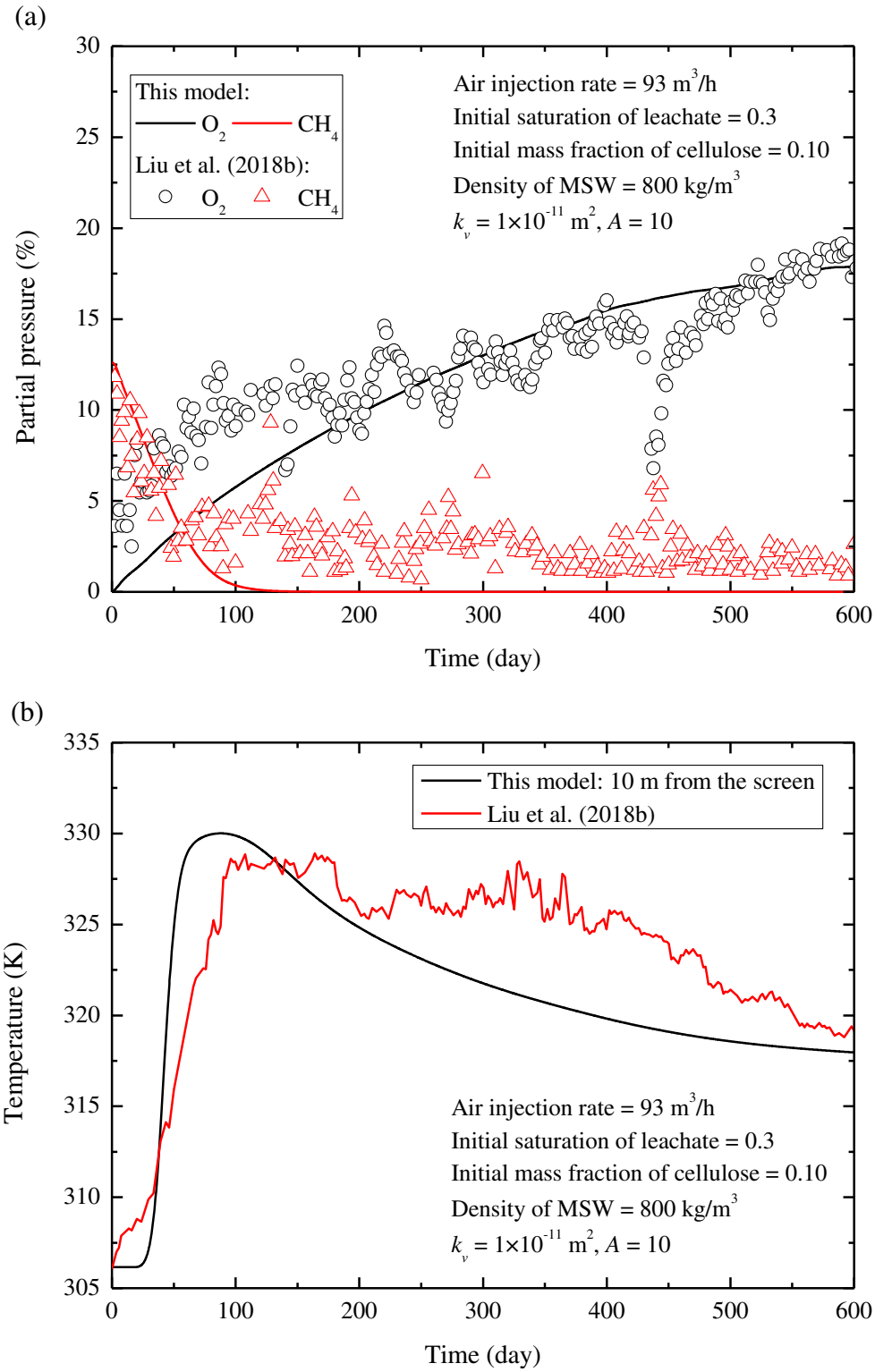

Fig. 3 Comparison between the simulation results and the in situ data reported by Liu et al. (2018b). **a** Partial pressures of O_2 and CH_4. **b** Temperature

rapidly to a peak value of 0.163 mol L^{-1} in the first 100 days (Fig. 8b) because of a relatively strong hydrolysis reaction (AN_I). It then significantly decreases to a concentration lower than 0.01 mol L^{-1} and maintains this level over time due to an increased concentration of X_{ANII}, which is several thousand times the initial value. The same tendency for VFA curve has also been reported by McDougall (2007) and Kim et al. (2007). Besides, the peak of methanation biomass (X_{ANII}) concentration occurs about 400 − 350 = 50 days later than that of hydrolysis biomass (X_{ANI}) concentration.

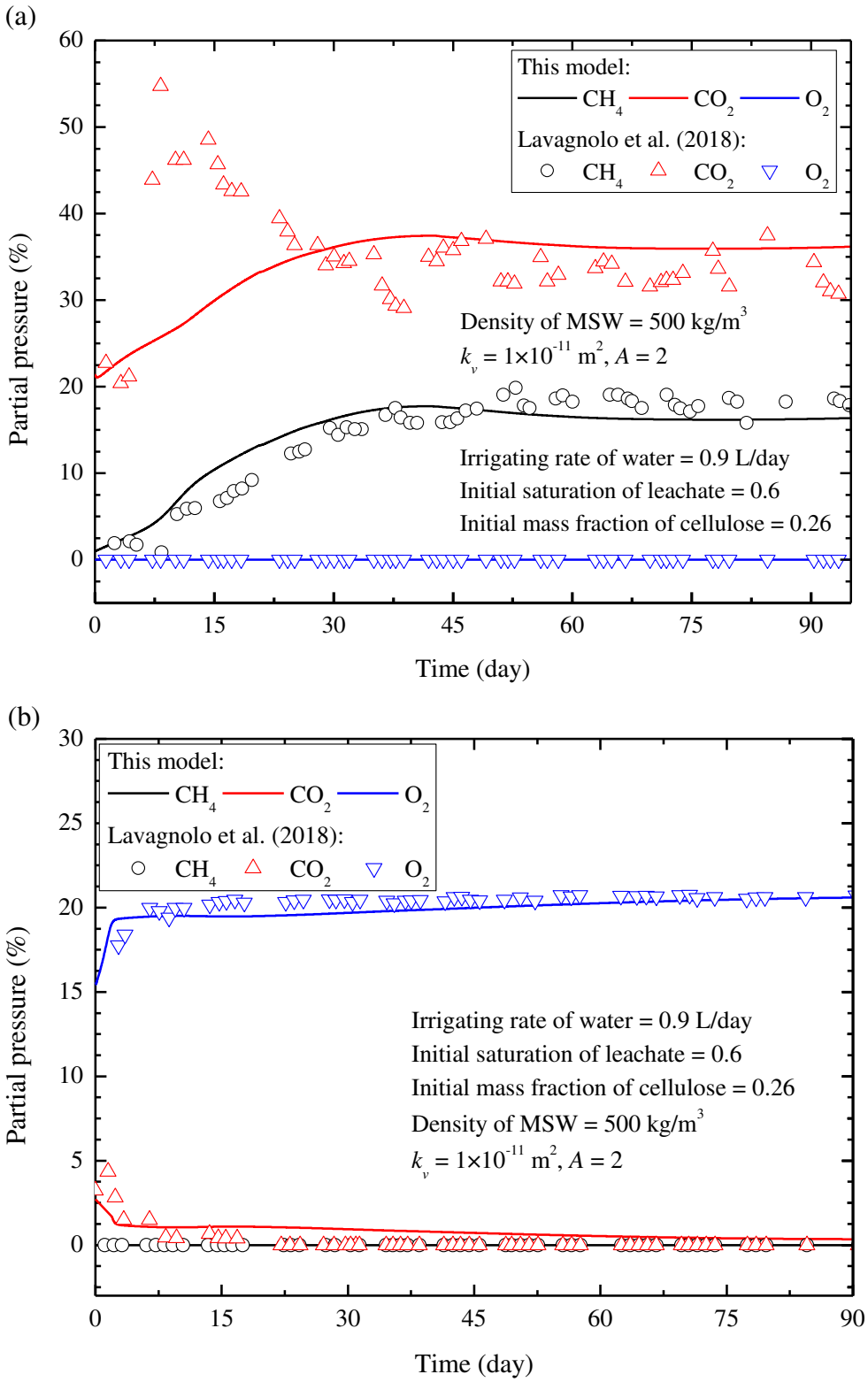

Fig. 4 Comparison between the simulation results and the laboratory test data reported by Lavagnolo et al. (2018). **a** Partial pressures of different components under anaerobic condition. **b** Partial pressures of different components under aerobic condition

Influence of intrinsic permeability and aeration pressure

Intrinsic permeability, measured by in situ or laboratory tests (Powrie and Beaven 1999; Stoltz et al. 2010), is the most important parameter that affects the fluid flow in waste and hence the efficiency of low pressure aeration. It should be noted that the intrinsic permeability mainly decreases with an increasing degree of compaction (Reddy et al. 2009). The change in porosity caused by

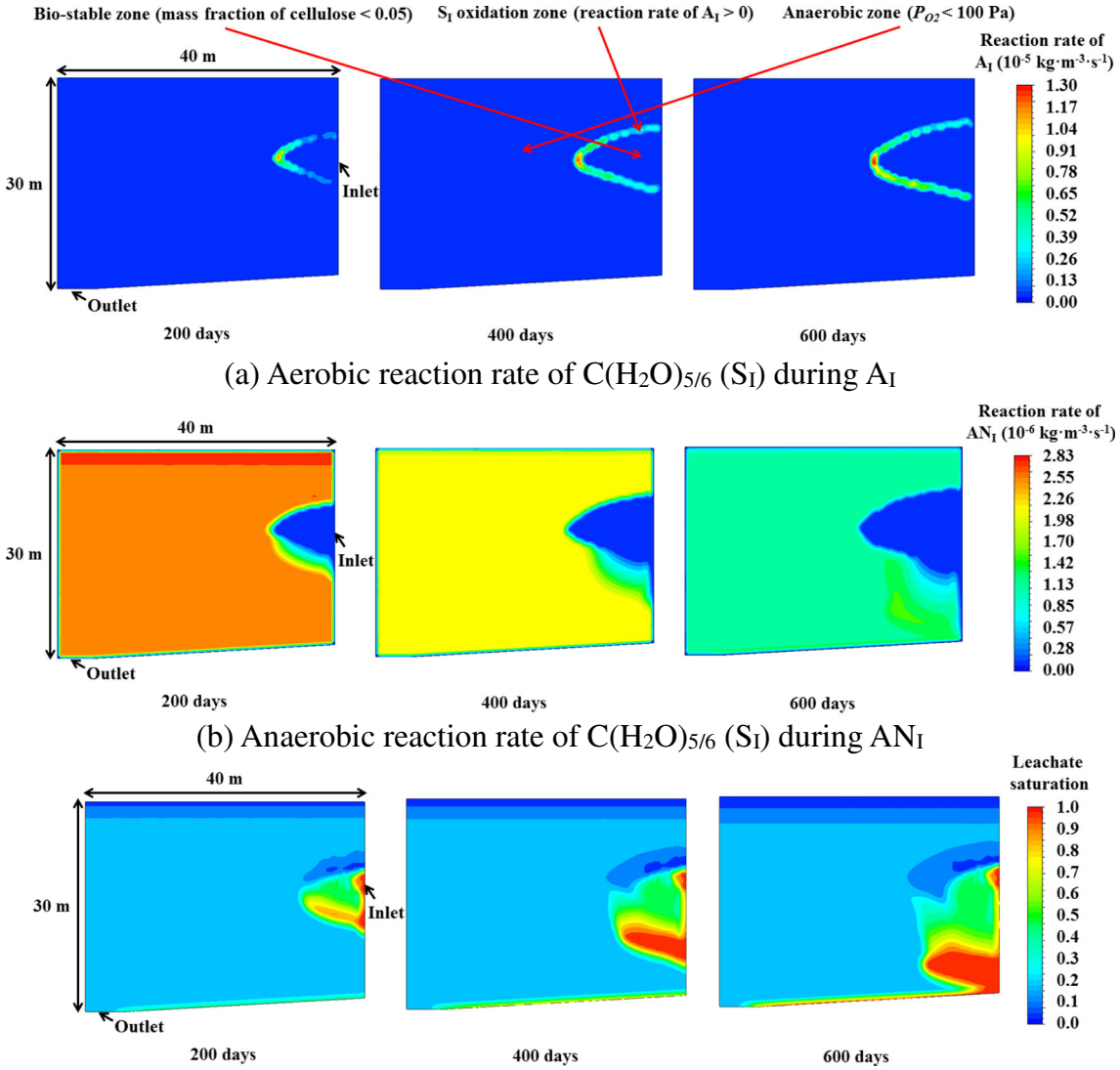

Fig. 5 Temporal and spatial distributions of **a** reaction rate of A_I, **b** reaction rate of AN_I, and **c** leachate saturation

biodegradation also alters the intrinsic permeability. However, since the composition and settlement of MSW in old landfills are nearly stable (Townsend et al. 2015; Hrad and Huber-Humer 2017; Liu et al. 2018b), the intrinsic permeability slightly changes during aeration. Thus, the intrinsic permeability is assumed to be constant during aeration. For an aeration pressure of 6 kPa, the bio-stable zone increases with an increase in k_v from 10^{-13} to 10^{-10} m^2 as expected (Fig. 9a). When k_v is equal to 10^{-13} m^2, the horizontal range of bio-stable zone (D_{hs}) is lower than 8 m after aeration for 1000 days, which would induce an accumulation of oxygen and an increased pressure impeding oxygen injection, giving a risk of high temperature. The D_{hs} increases to about 22 m for $k_v = 10^{-11}$ m^2 and 27 m for $k_v = 10^{-10}$ m^2 after aeration for 1000 days. For the total oxygen consumption rate of cellulose oxidation (A_I), it increases over time at a decreased rate and then decreases due to a significant consumption of cellulose, especially for $k_v > 10^{-11}$ m^2 (Fig. 9b). The maximum oxygen consumption rate decreases from 0.22 to 0.01 L s^{-1} as k_v decreases from 10^{-10} to 10^{-13} m^2 which further confirms the inefficiency of aeration when k_v was equal to 10^{-13} m^2. Thus, air injection is not suggested if k_v is lower than 10^{-13} m^2.

A low pressure of 2 kPa to 8 kPa is suggested for aeration by Ritzkowski and Stegmann (2012) and has been widely used in aerobic landfills (Ritzkowski and Stegmann 2013; Raga and Cossu 2014; Hrad and Huber-Humer 2017). With an increase in aeration pressure, the horizontal range of bio-stable zone at $t = 1000$ days increases as expected (Fig. 10), and almost linear curves

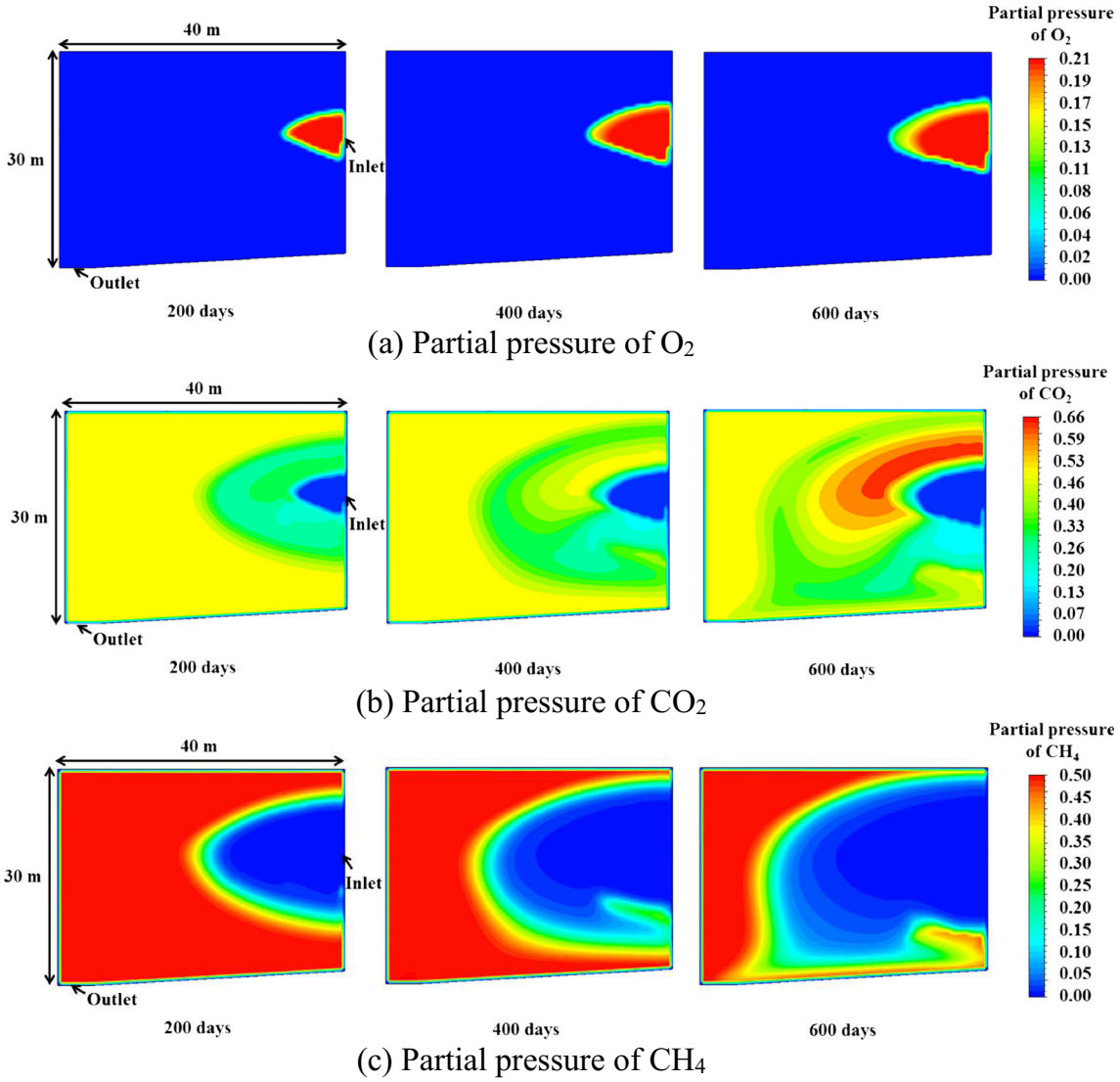

Fig. 6 Temporal and spatial distributions of partial pressures of **a** O_2, **b** CO_2, and **c** CH_4

are observed. In the rest part, an injection pressure of 6 kPa is used.

In Fig. 10, another scenario is also investigated, namely the anaerobic reactions AN_I (hydrolysis), AN_{II} (methanation), and AN_{III} (methanation) that are turned off. The comparison of results between the scenario considering anaerobic biodegradation and that without considering anaerobic biodegradation reveals that D_{hs} is significantly underestimated if all celluloses in waste are oxidized directly by the injected oxygen without anaerobic biodegradation processes. The fact in aerobic landfills is that part of cellulose is hydrolyzed first (AN_I) and then the products of anaerobic biodegradation (VFA and CH_4) are oxidized (A_{II} and A_{IV}). Compared with cellulose being oxidized directly, the oxidation rates of VFA and CH_4 are much faster, which means that anaerobic biodegradation is essential for the simulation of aeration in landfills.

Influence of vertical well depth

Closed landfills are generally tens of meters deep, and arranging aeration VWs at different depths would allow the development of an even distribution of injected oxygen in the vertical direction. The shape of bio-stable zone varies with different VW depths due to the existence of landfill boundaries. Figure 11 gives the horizontal and vertical ranges of bio-stable zone for H_w/H_0 = 0.2, 0.4, 0.6, and 0.8 (H_s/H_w = 0.1 and elapsed time = 1000 days). The horizontal range (D_{hs}) essentially remains stable around 17.5 m until $H_w/H_0 > 0.6$ and then increases to 19.8 m for H_w/H_0 = 0.8 because the bottom liner system obstructs the gas flow in vertical direction. For the vertical range (D_{vs}), it increases to a maximum value of 13.4 m at H_w/H_0 = 0.4 and then gradually decreases to 10.3 m at H_w/H_0 = 0.8 due to the obstruction of gas induced by bottom

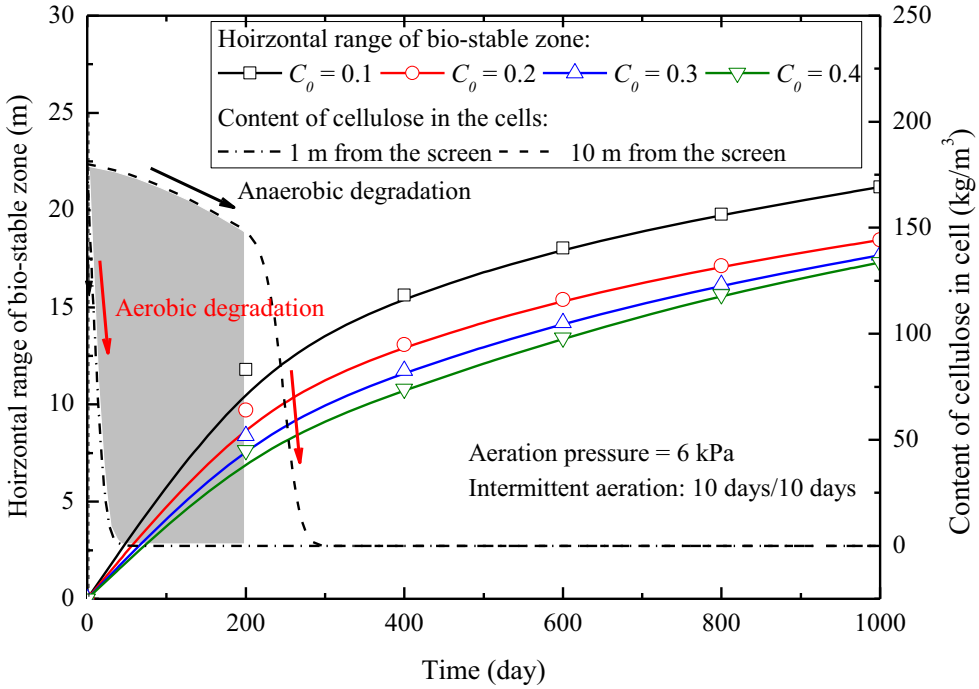

Fig. 7 Temporal variations of the horizontal range of bio-stable zone for four values of the initial mass fraction of cellulose (0.1 to 0.4) and the cellulose content of the cells with a horizontal distance of 1 m and 10 m away from the well screen (initial mass fraction of cellulose = 0.3)

boundary. Thus, a horizontal spacing of 17 m is suggested for aeration VWs with a vertical spacing of 10 m for screens in Fig. 11.

Influence of aeration frequency

Intermittent aeration combined with leachate recirculation has proved to be an appropriate option for aerobic bioreactor landfills (Powell et al. 2006; Öncü et al. 2012; Tran et al. 2014; Townsend et al. 2015; Nag et al. 2018) since leachate recirculation can decrease waste temperature and guarantee the essential moisture content for aerobic biodegradation. The temperature of waste will increase with the duration of aeration which has an adverse impact on the safety of landfills; thus, aeration frequency is an important design parameter. On the other hand, aeration with a too high frequency has proved to be inefficient because too much recirculated leachate would obstruct gas flow in waste.

Within 1 cycle of aeration and recirculation (1:1), the maximum temperature in landfills generally increases during aeration and then decreases during recirculation (Fig. 12a). For an aeration duration of 50 days, there is a decrease in the maximum temperature before leachate recirculation mainly due to the expansion of aerobic zone (Fig. 5a) and hence heat transfers into a low-temperature region easily. Using an intermittent aeration of 20 days/20 days and 50 days/50 days, the maximum temperature would increase to a peak of 328 K by about 20 K in Fig. 12a, while the peak value is 324 K when the duration of aeration is 10 days. In terms of explosion, this temperature (328 K) is relatively safe (Townsend et al. 2015) but operators should pay attention to the increase in temperature because the initial temperature in landfills may be higher than 308 K. The decrease in maximum temperature during leachate recirculation is significant when using aeration frequencies of 10 days/10 days and 20 days/20 days (about 8 K). However, the cooling effect is unsatisfactory when the duration of aeration is 50 days, and the maximum temperature only drops by 3 K during the recirculation stage because, when aeration time is 50 days, the aerobic zone is too big and leachate cannot cool the whole high-temperature zone during the recirculation stage.

With a decrease in aeration frequency from 5 days/5 days to 50 days/50 days, the cumulative oxygen consumption by reaction A_I shows an increase by 38% in 800 days (Fig. 12b). During recirculation, the oxygen consumption almost remains unchanged (enlarged view in Fig. 12b) and the leachate saturation increases. However, when aeration restarts, the aeration pressure would make the recirculated leachate flow away, which is called "leachate re-discharge." A higher frequency (i.e., scenario of 5 days/5 days) of leachate re-discharge caused by aeration pressure would impede oxygen flow and hence cellulose oxidation and oxygen consumption. Therefore, a lower aeration frequency is preferred in terms of aeration efficiency.

The horizontal range of bio-stable zone (D_{hs}) increases with an increase in the duration of aeration (Fig. 13), namely a decrease in aeration frequency, which is consistent with the results in Fig. 12b. D_{hs} significantly increases with the aeration duration increases from 5 days to 20 days and then only slightly increases with a further increase of aeration duration.

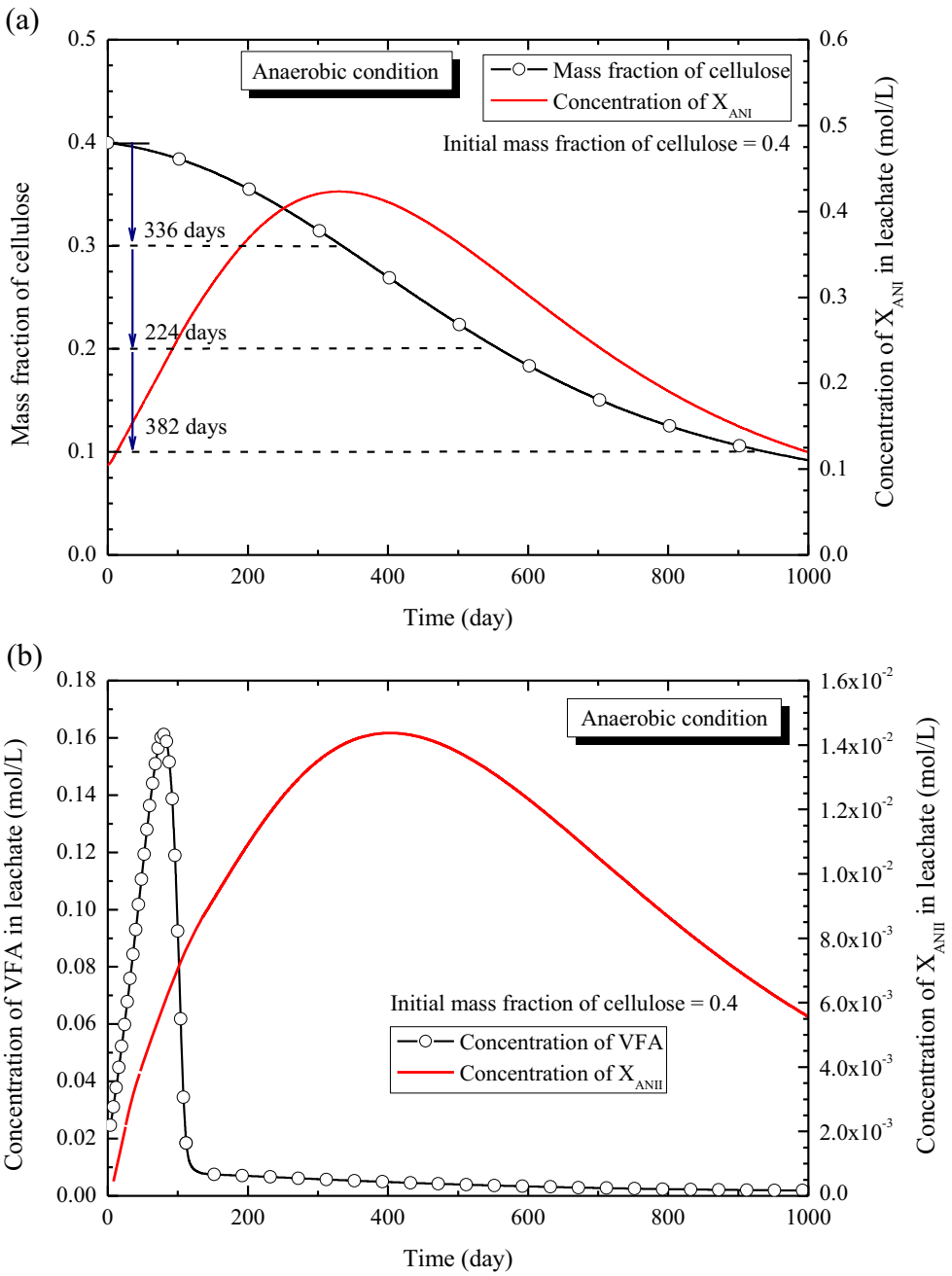

Fig. 8 Temporal changes in the **a** mass fraction of cellulose and concentration of X_{ANI} and **b** concentrations of VFA and X_{ANI}, in a cell located at 40 m horizontally away from the well screen (completely anaerobic condition)

Considering that aeration is more effective in accelerating biodegradation compared to leachate recirculation, the duration of aeration could be increased, giving another operation pattern: aeration/leachate recirculation is 1:0.5. The D_{hs} increases by about 3 m in average using this operation pattern. Nevertheless, a greater proportion of aeration duration would weaken the cooling effect of leachate recirculation and give rise to a risk of explosion due to the increased temperature.

Based on the above analysis, an intermittent aeration of 50-day aeration/50-day leachate recirculation might give a high temperature incurring a security risk (Fig. 12a) and the aeration efficiency of 20 days/20 days is better than that of 5 days/5 days and 10 days/10 days (Fig. 13). Thus, an aeration frequency of 20 days/20 days is recommended in terms of safety and efficiency and, when landfills are wet with relatively low temperature, the proportion of aeration can be increased to 0.67 (i.e., 20-day aeration/10-day recirculation) or an even higher value.

Summary and conclusions

In this study, a numerical model, which couples aerobic-anaerobic biodegradation, multi-phase flow, multi-

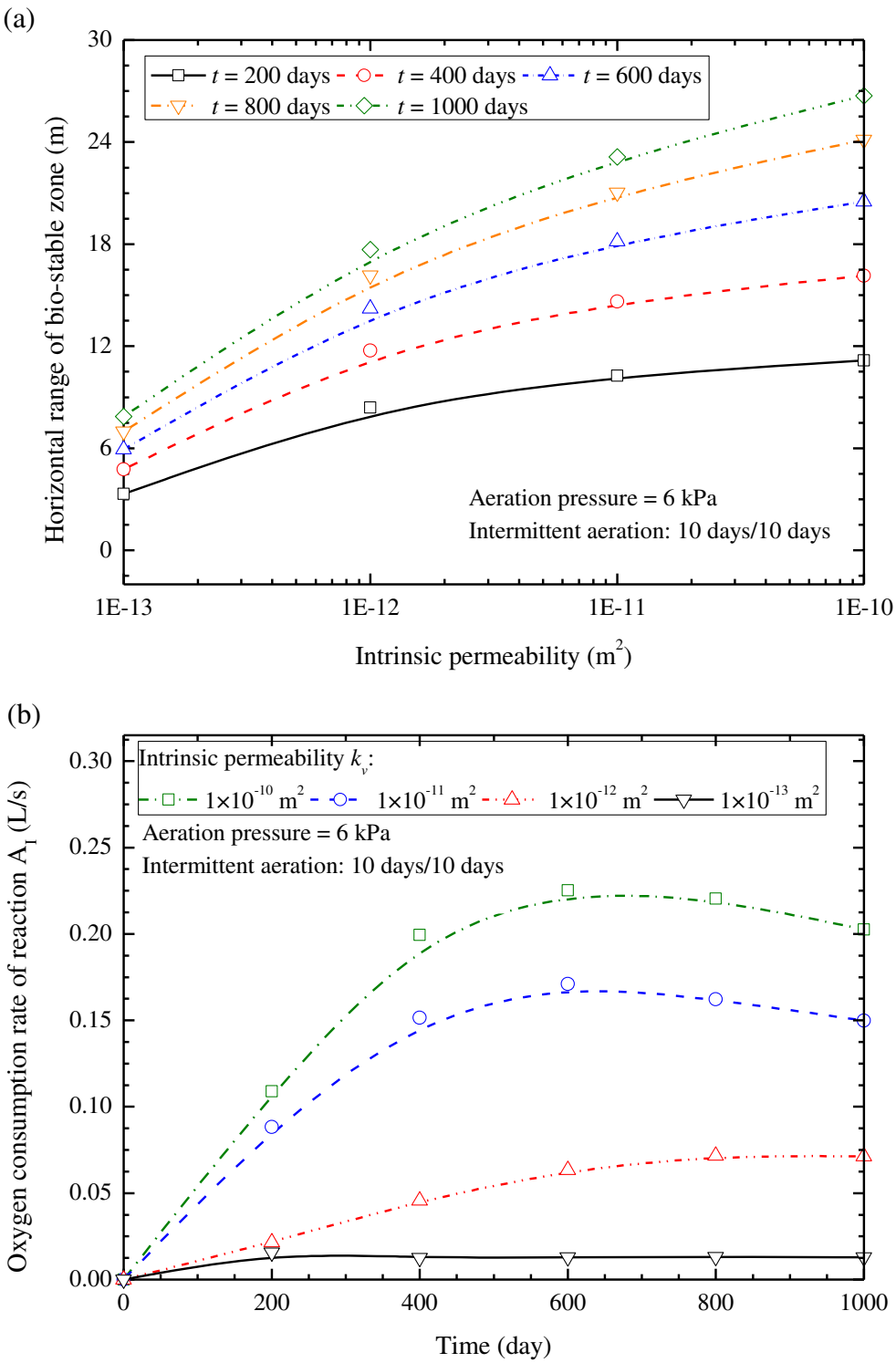

Fig. 9 Relationships between the **a** horizontal range of bio-stable zone and waste intrinsic permeability and the **b** oxygen consumption rate of cellulose oxidation and time

component transport, and heat transfer, is developed using a computational fluid dynamics (CFD) technique. After being verified using existing in situ and laboratory test results, the model is then employed to reveal the bio-stable zone development, aerobic biochemical reactions around vertical well (VW), and anaerobic reactions away from VW. Some conclusions can be drawn as follows:

1. The horizontal range of bio-stable zone increases with a decrease in the initial mass fraction of cellulose (C_0). The

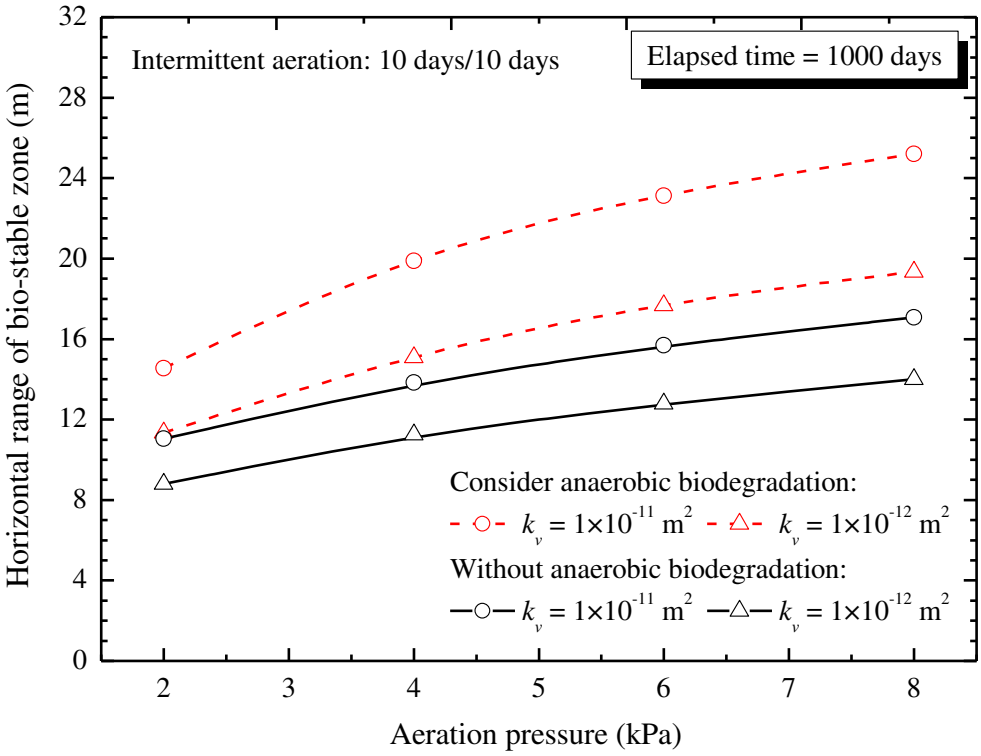

Fig. 10 Variations of the horizontal range of bio-stable zone with aeration pressure for different intrinsic permeabilities and comparison with the cases without anaerobic biodegradation

time needed to reach a horizontal range of 15 m is 400 days for $C_0 = 0.1$, which is half of the time for $C_0 = 0.4$.

2. When the waste intrinsic permeability is equal or greater than 10^{-11} m^2, aeration using a low pressure between 4 and 8 kPa is appropriate, giving a horizontal range of bio-stable zone larger than 18 m. However, low-pressure aeration is not effective for $k_v \leq 10^{-13}$ m^2 with a horizontal range less than 8 m.

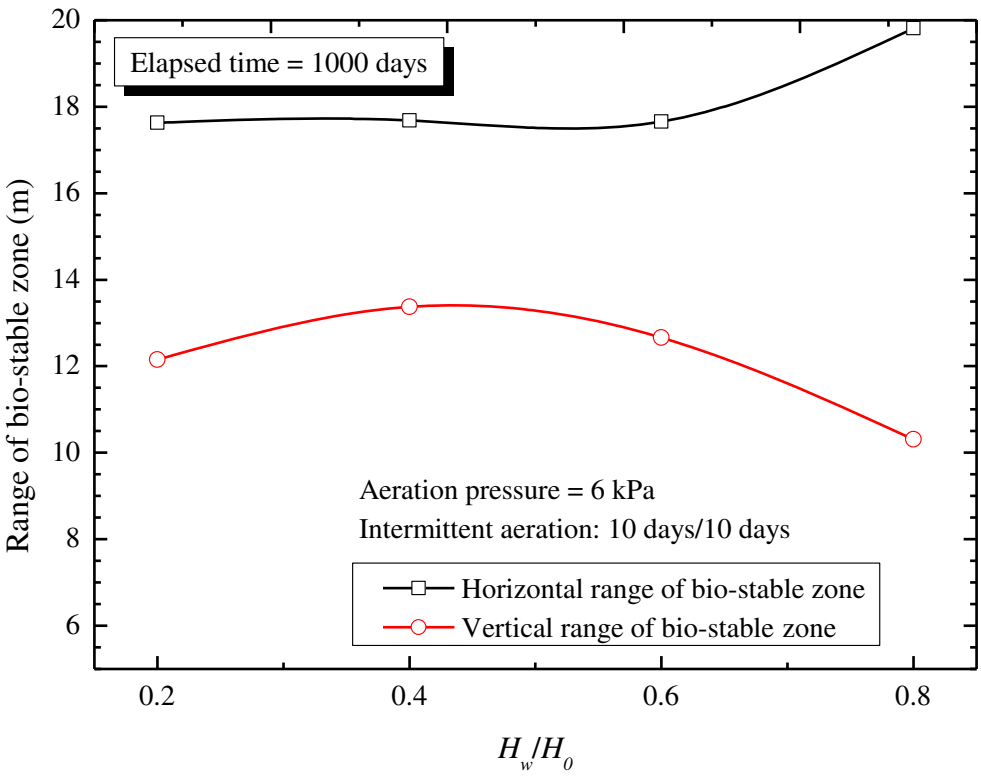

Fig. 11 Range of zone where bio-stability is reached under different H_w/H_0 values

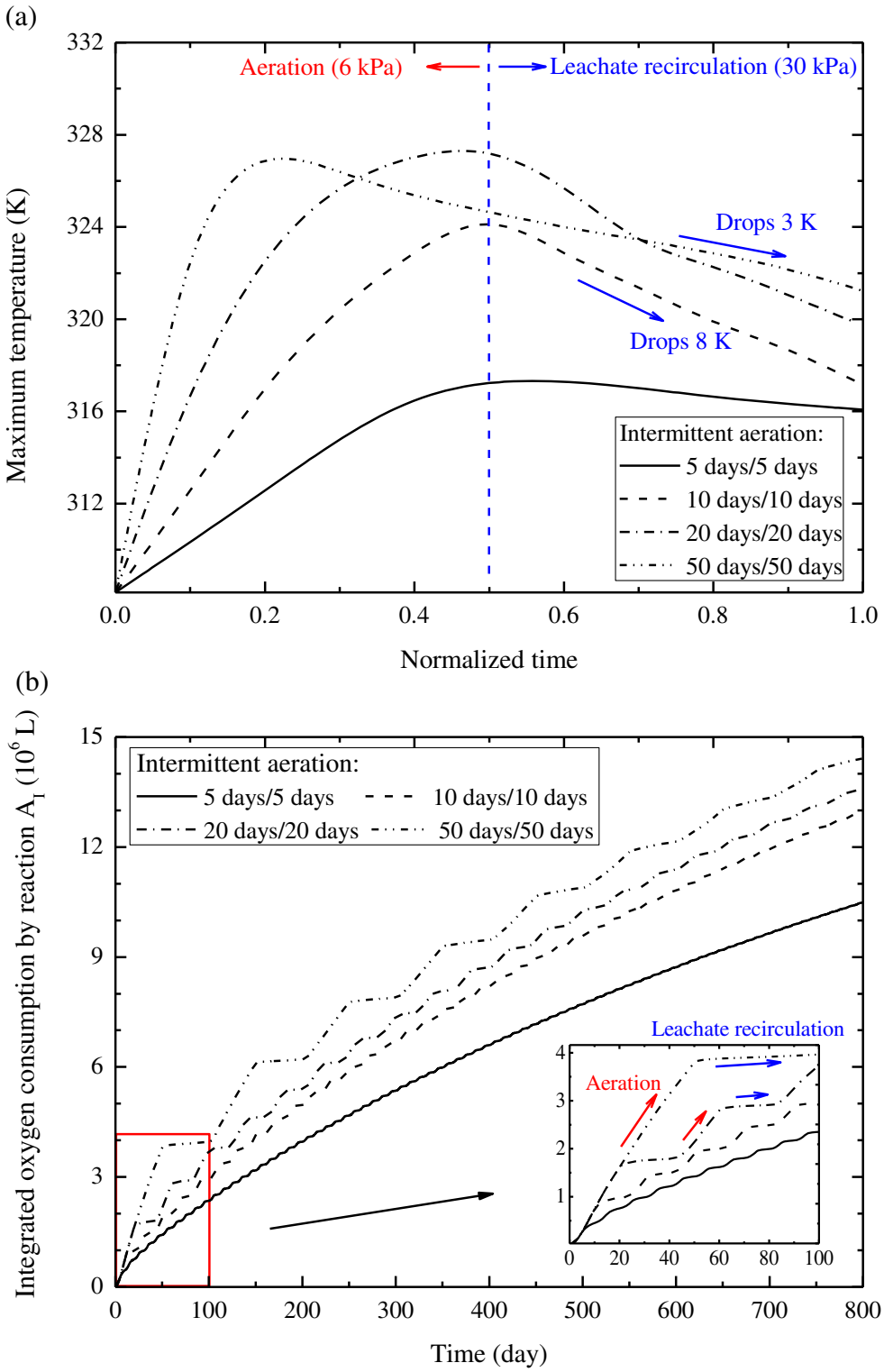

Fig. 12 Variation of the **a** maximum temperature and **b** integrated oxygen consumption in waste under different aeration frequencies

3. With an increase in aeration pressure, the horizontal range of bio-stable zone at t = 1000 days increases as expected, and almost linear curves are observed. The aeration efficiency would be underestimated if anaerobic biodegradation is neglected because products of anaerobic biodegradation processes would be oxidized more easily than cellulose.
4. An impermeable cover at the top and liner at the bottom would impede gas flow in vertical direction, especially when the injection screen of vertical wells approaches

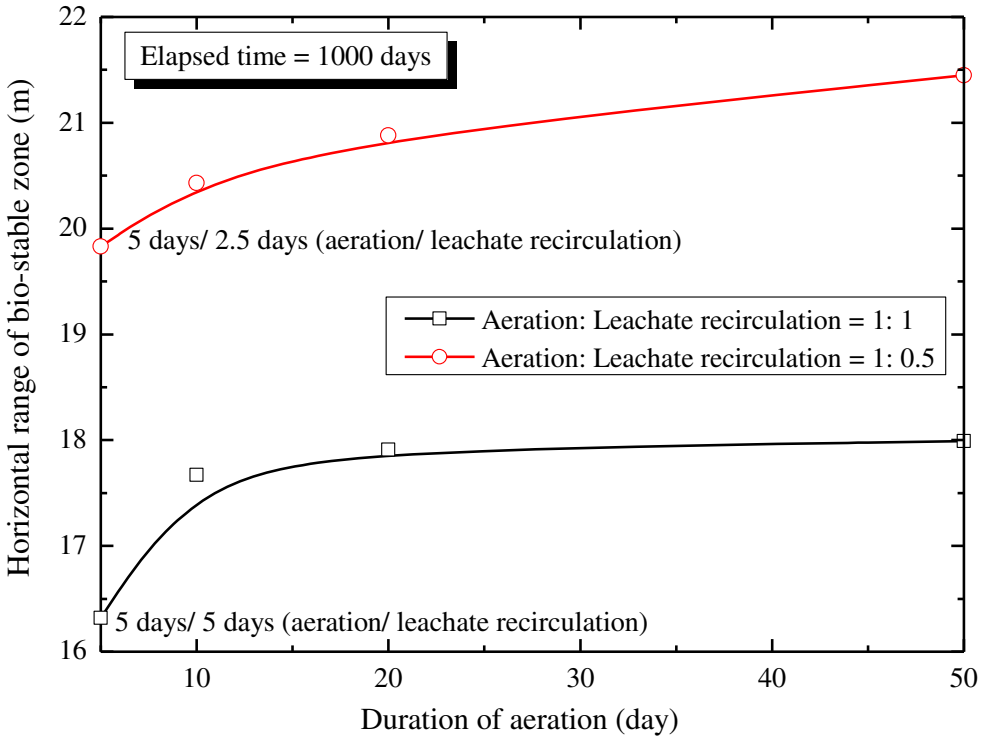

Fig. 13 Variation of the horizontal range of bio-stable zone under different aeration patterns

the top or bottom of landfills. A horizontal spacing of 17 m is suggested for aeration VWs with a vertical spacing of 10 m for screens.

5. For intermittent aeration, operators should balance the aeration efficiency and the threat of high temperature. Thus, an aeration frequency of 20-day aeration/20-day recirculation is preferred. For wet landfills with low temperature, the proportion of aeration can be increased to 0.67 (20-day aeration/10-day recirculation) or an even higher value.

Notations

$\tau^{=}$ shear stress tensor
Aanisotropy of MSW
$D_i$mass diffusion coefficient for component i
$D_{T,i}$thermal diffusion coefficient
$f_T$inhibition factor of temperature
$f_\theta$inhibition factor of moisture content
$g$acceleration of gravity
H_0landfill height
$H_s$screen length of VW
H_wVW depth
$h_q$specific enthalpy of phase q
$\overrightarrow{J_i}$ diffusion flux of component i
$k_i$intrinsic permeability
$k_\bullet$Monod saturation constant
$k_{O2,i}$saturation constant of O_2
k_{CH4}saturation constant for CH_4
$k_r$relative permeability
$K_\bullet$reaction rate constant
m_{vg}van Genuchten constant
$n$total porosity of MSW
n_{vg}van Genuchten constant
$p_q$liquid/gas pressure
$p_c$capillary pressure
P_{O_2} partial pressure of O_2
P_{H2}partial pressure of H_2
P_{CH4}partial pressure of CH_4
$q_q$heat flux
Q_{pq}intensity of heat exchange between phases
$R_\bullet^i$ reaction rate
$R_i$source/sink term of component i in biochemical reactions
$R_\bullet^D$ decay rate of biomass
$S_i$concentration of substrate
$S_e$effective degree of saturation
$S_q$source/sink term of phase q
$t$time
Ttemperature
$V_q$volume occupied by phase q
$\overrightarrow{v_q}$ velocity of phase q
$X_\bullet$concentration of biomass
$X_\bullet^{ini}$ initial concentration of biomass
$Y_i$mass fraction of component i in phase q
$Y_\bullet$yield coefficient
α_{lr}residual volume fraction of leachate phase
α_{ls}maximum volume fraction of leachate phase
$\alpha_q$phasic volume fraction of phase q
α_{vg}VGM parameter related to the gas entry pressure
$\mu_q$dynamic viscosity of phase q
$\mu_\bullet$specific growth rate of biomass
$\mu_\bullet^{max}$ maximum specific growth rate
$\eta_\bullet$environmental inhibition factor
$\rho_q$density of phase q

Funding information The work was supported by the National Natural Science Foundation of China under Grant Nos. 41725012, 41572265, and 41661130153; the Shuguang Scheme under Grant No. 16SG19; and the Newton Advanced Fellowship of the Royal Society under Grant No. NA150466.

References

ANSYS (2009) ANSYS Fluent 12.0 user's guide. Canonsburg, PA: ANSYS

Cao BY, Feng SJ, Li AZ (2018) CFD modeling of anaerobic-aerobic hybrid bioreactor landfills. Int J Geomech 18:04018072

Feng SJ, Lu SF, Chen HX, Fu WD, Lü F (2017a) Three-dimensional modelling of coupled leachate and gas flow in bioreactor landfills. Comput Geotech 84:138–151

Feng SJ, Gao KW, Chen YX, Li Y, Zhang LM, Chen HX (2017b) Geotechnical properties of municipal solid waste at Laogang Landfill, China. Waste Manag 63:354–365

Feng SJ, Cao BY, Li AZ, Chen HX, Zheng QT (2018) CFD modeling of hydro-biochemical behavior of MSW subjected to leachate recirculation. Environ Sci Pollut Res 25:5631–5642

Fytanidis DK, Voudrias EA (2014) Numerical simulation of landfill aeration using computational fluid dynamics. Waste Manag 34:804–816

Grisey E, Aleya L (2016) Prolonged aerobic degradation of shredded and pre-composted municipal solid waste: report from a 21-year study of leachate quality characteristics. Environ Sci Pollut Res 23(1):800–815

Haarstrick A, Mora-Naranjo N, Meima J, Hempel DC (2004) Modeling anaerobic degradation in municipal landfills. Environ Eng Sci 21(4): 471–484

Hrad M, Huber-Humer M (2017) Performance and completion assessment of an in-situ aerated municipal solid waste landfill—final scientific documentation of an Austrian case study. Waste Manag 63: 397–409

Hubert J, Liu X, Collin F (2016) Numerical modeling of the long term behavior of municipal solid waste in a bioreactor landfill. Comput Geotech 72:152–170

Kim SY, Tojo Y, Matsuto T (2007) Compartment model of aerobic and anaerobic biodegradation in a municipal solid waste landfill. Waste Manag Res 25:524–537

Ko JH, Powell J, Jain P, Kim H, Townsend T, Reinhart D (2013) Case study of controlled air addition into landfilled municipal solid waste: design, operation, and control. J Hazard Toxic Radioact Waste 17: 351–359

Lavagnolo MC, Grossule V, Raga R (2018) Innovative dual-step management of semi-aerobic landfill in a tropical climate. Waste Manag 74:302–311

Liu L, Ma J, Xue Q, Wan Y, Yu X (2018a) Modeling the oxygen transport process under preferential flow effect in landfill. Environ Sci Pollut Res 25:18559–18569

Liu L, Ma J, Xue Q, Shao J, Chen Y, Zeng G (2018b) The in situ aeration in an old landfill in China: multi-wells optimization method and application. Waste Manag 76:614–620

McDougall J (2007) A hydro-bio-mechanical model for settlement and other behaviour in landfilled waste. Comput Geotech 34:229–246

Nag M, Shimaoka T, Komiya T (2018) Influence of operations on leachate characteristics in the aerobic-anaerobic landfill method. Waste Manag 78:698–707

Ng CWW, Feng S, Liu H (2015) A fully coupled model for water-gas-heat reactive transport with methane oxidation in landfill covers. Sci Total Environ 508:307–319

Omar H, Rohani S (2017) The mathematical model of the conversion of a landfill operation from anaerobic to aerobic. Appl Math Model 50: 53–67

Öncü G, Reiser M, Kranert M (2012) Aerobic in situ stabilization of landfill Konstanz Dorfweiher: leachate quality after 1 year of operation. Waste Manag 32:2374–2384

Park JK, Chong YG, Tameda K, Lee NH (2018) Methods for determining the methane generation potential and methane generation rate constant for the FOD model: a review. Waste Manag Res 36:200–220

Powell J, Jain P, Kim H, Townsend T, Reinhart D (2006) Changes in landfill gas quality as a result of controlled air injection. Environ Sci Technol 40:1029–1034

Powrie W, Beaven R (1999) Hydraulic properties of household waste and implications for landfills. Proc Inst Civ Eng Geotech Eng 137:235–237

Raga R, Cossu R (2014) Landfill aeration in the framework of a reclamation project in Northern Italy. Waste Manag 34:683–691

Raga R, Cossu R, Heerenklage J, Pivato A, Ritzkowski M (2015) Landfill aeration for emission control before and during landfill mining. Waste Manag 46:420-429

Reddy KR, Hettiarachchi H, Parakalla N, Gangathulasi J, Bogner J, Lagier T (2009) Hydraulic conductivity of MSW in landfills. J Environ Eng 135:677–683

Reddy KR, Kulkarni HS, Khire MV (2012) Two-phase modeling of leachate recirculation using vertical wells in bioreactor landfills. J Hazard Toxic Radioact Waste 17:272–284

Reichenberger V, Jakobs H, Bastian P, Helmig R (2006) A mixed-dimensional finite volume method for two-phase flow in fractured porous media. Adv Water Resour 29:1020–1036

Ritzkowski M, Stegmann R (2012) Landfill aeration worldwide: concepts, indications and findings. Waste Manag 32:1411–1419

Ritzkowski M, Stegmann R (2013) Landfill aeration within the scope of post-closure care and its completion. Waste Manag 33:2074–2082

Ritzkowski M, Walker B, Kuchta K, Raga R, Stegmann R (2016) Aeration of the teuftal landfill: Field scale concept and lab scale simulation. Waste Management 55:99-107

Stoltz G, Gourc JP, Oxarango L (2010) Liquid and gas permeabilities of unsaturated municipal solid waste under compression. J Contam Hydrol 118:27–42

Townsend TG, Powell J, Jain P, Xu Q, Tolaymat T, Reinhart D (2015) Sustainable practices for landfill design and operation. Springer, New York

Tran HN, Münnich K, Fricke K, Harborth P (2014) Removal of nitrogen from MBT residues by leachate recirculation in combination with intermittent aeration. Waste Manag Res 32:56–63

White J (2008) The application of LDAT to the HPM2 challenge. Proceedings of the Institution of Civil Engineers-Waste and Resource Management Thomas Telford Ltd, pp. 137-146

White J, Zardava K, Nayagum D, Powrie W (2015) Functional relationships for the estimation of van Genuchten parameter values in landfill processes models. Waste Manag 38:222–231